Autophagy 8:9, 1357-1370; September 2012; © 2012 Landes Bioscience

ESX-1 dependent impairment of autophagic flux by *Mycobacterium tuberculosis* in human dendritic cells

Alessandra Romagnoli,[1] Marilena P. Etna,[2] Elena Giacomini,[2] Manuela Pardini,[2] Maria Elena Remoli,[2] Marco Corazzari,[1] Laura Falasca,[1] Delia Goletti,[1] Valérie Gafa,[2] Roxane Simeone,[4] Giovanni Delogu,[3] Mauro Piacentini,[1,5] Roland Brosch,[4] Gian Maria Fimia[1,*] and Eliana M. Coccia[2,*]

[1]Department of Epidemiology and Preclinical Research; National Institute for Infectious Diseases "L. Spallanzani"; Rome, Italy; [2]Department of Infectious, Parasitic and Immune-mediated Diseases; Istituto Superiore di Sanità; Rome, Italy; [3]Istituto di Microbiologia; Università Cattolica del Sacro Cuore; Rome, Italy; [4]Institut Pasteur; Unité de Pathogénomique Mycobactérienne Intégrée; Paris, France; [5]Department of Biology; University of Rome "Tor Vergata"; Rome, Italy

Keywords: *Mycobacterium tuberculosis*, BCG, RD1 region, ESX1/type VII secretion system, vaccine, autophagy, dendritic cells

Abbreviations: ADC, albumin, dextrose, catalase; Ag85B, antigen 85 B; BCG, Bacillus Calmette-Guerin; CTSB, cathepsin B; CBA, cytometric bead assay; CD, cluster of differentiation; CFP-10, 10 kD culture filtrate protein; CFU, colony forming units; Cy, cyanine; DC, dendritic cells; DMSO, dimethyl sulfoxide; ECL, enhanced chemiluminescence; ESAT-6, 6 kD early secreted antigenic target; ESX-1, ESAT-6 secretion system-1; FITC, fluorescein isothiocyanate; FCS, fetal calf serum; GAPDH, glyceraldehyde-3-phosphate dehydrogenase; CSF2/GM-CSF, granulocyte-macrophage colony stimulating factor; HLA-DR, human leucocytes antigen-DR; IF, immunofluorescence; IFN, interferon; IL, interleukin; LAMP1, lysosomal-associated membrane protein 1; MAP1LC3/LC3, microtubule-associated protein 1A/1B-light chain 3; LPS, lipopolysaccharide; MDR-TB, multidrug-resistant tuberculosis; MHC, major histocompatibility complex; MLR, mixed lymphocyte reaction; MOI, multiplicity of infection; mRNA, messenger RNA; Mtb, *Mycobacterium tuberculosis*; MTOR, mechanistic target of rapamycin; OADC, oleic acid albumin dextrose complex; PAF, paraformaldehyde; PBMC, peripheral blood mononuclear cell; PBS, phosphate buffered saline; PE, phycoerythrin; pepA, pepstatin A; PVDF, polyvinylidene fluoride; Rapa, rapamycin; RD1, region of differentiation 1; RT-PCR, real time-polymerase chain reaction; SapM, secreted acid phosphatase of *Mycobacterium tuberculosis*; SE, standard error; SEM, standard error of the mean; SQSTM1/p62, sequestosome 1; TB, tuberculosis; TBS, tris buffered saline; Th, T helper; TNF, tumor necrosis factor-α; WB, western blot; XDR-TB, extensively-drug-resistant tuberculosis

Emerging evidence points to an important role of autophagy in the immune response mediated by dendritic cells (DC) against *Mycobacterium tuberculosis* (Mtb). Since current vaccination based on Bacillus Calmette-Guerin (BCG) is unable to stop the tuberculosis epidemic, a deeper comprehension of the alterations induced by Mtb in DC is essential for setting new vaccine strategies. Here, we compared the capacity of virulent (H37Rv) and avirulent (H37Ra) Mtb strains as well as BCG to modulate autophagy in human primary DC. We found that Mtb H37Rv impairs autophagy at the step of autophagosome-lysosome fusion. In contrast, neither Mtb H37Ra nor BCG strains were able to hamper autophagosome maturation. Both these attenuated strains have a functional inhibition of the 6kD early secreted antigenic target ESAT-6, an effector protein of the ESAT-6 Secretion System-1(ESX-1)/type VII secretion system. Notably, the ability to inhibit autophagy was fully restored in recombinant BCG and Mtb H37Ra strains in which ESAT-6 secretion was re-established by genetic complementation using either the ESX-1 region from Mtb (BCG::ESX-1) or the PhoP gene (Mtb H37Ra::PhoP), a regulator of ESAT-6 secretion. Importantly, the autophagic block induced by Mtb was overcome by rapamycin treatment leading to an increased interleukin-12 expression and, in turn, to an enhanced capacity to expand a Th1-oriented response. Collectively, our study demonstrated that Mtb alters the autophagic machinery through the ESX-1 system, and thereby opens new exciting perspectives to better understand the relationship between Mtb virulence and its ability to escape the DC-mediated immune response.

Introduction

Tuberculosis (TB) is still a leading cause of death worldwide despite the availability of the Bacillus Calmette-Guerin (BCG) vaccine and specific antibiotic treatments. The currently used BCG vaccine, based on a live attenuated strain of *Mycobacterium bovis*, offers variable protection efficacy and therefore needs to be either improved or replaced.[1] Different TB vaccine candidates

*Correspondence to: Gian Maria Fimia and Eliana M. Coccia; Email: gianmaria.fimia@inmi.it and eliana.coccia@iss.it
Submitted: 01/07/12; Revised: 05/17/12; Accepted: 05/25/12
http://dx.doi.org/10.4161/auto.20881

involving recombinant BCG, subunit vaccine and live attenuated *Mycobacterium tuberculosis* (Mtb) strains are currently under investigation.[2] Comparative genomics of the Mtb complex revealed that the attenuation of BCG is related to the loss of the protein secretion system ESX-1 due to deletion of the region of difference 1 (RD1) locus.[3] This segment is localized close to the origin of replication in all fully virulent members of the complex and harbors genes *esxA* (Rv3875), coding for the 6-kDa early secreted antigenic target (ESAT-6), and *esxB* (Rv3874), encoding the 10-kDa culture filtrate protein (CFP-10).[4] ESAT-6 and CFP-10 are secreted via a member of type VII secretion system ESX-1, a dedicated secretion apparatus encoded by genes flanking *esxA* and *esxB* in the extended RD1 region.

A complex network of interactions between the host and pathogen controls the final outcome of Mtb infection.[5] After phagocytosis, Mtb persists within macrophages through a variety of immune evasion strategies, such as preventing the recognition of infected macrophages by T cells and inhibiting phagosome maturation.[6] Among several mechanisms used by the host to fight Mtb, the induction of the autophagic process represents a crucial step,[7-11] which can lead to both the killing of mycobacteria and the production of Mtb peptides and lipids for antigen presentation pathways.[12,13] An elegant indication of the role played by autophagy in reducing the viability of intracellular mycobacteria has been recently provided by Kumar and colleagues, who showed by means of a genome-wide RNA interference approach that the silencing of molecules involved in the process of autophagy enhanced the intracellular viability of Mtb.[14]

Autophagy functions in diverse aspects of innate and adaptive immunity mainly involved in the defense against intracellular pathogens.[15-18] In addition to the well-characterized role of autophagy in regulating the major histocompatibility complex (MHC) class II presentation of cytoplasmic and nuclear antigens, and of those obtained from phagocytosed pathogens, this process has been shown to provide novel routes for MHC class I antigen presentation and enhanced $CD8^+$ T-cell responses, for cross-presentation of dendritic cells (DC) to $CD8^+$ T cells.[19,20]

DC display peculiar features in respect to autophagy since a high constitutive activity has been observed,[21] which continuously provides peptidic antigens for MHC class II presentation in order to induce immunity or tolerance by immature and mature DC, respectively. In line with these findings, Jagannath and collaborators showed that in a mouse model the stimulation of autophagy by rapamycin enhanced the capacity of DC to present mycobacterial antigens into the MHC class II complex.[13]

Given the critical role played by DC in the regulation of the immune response against Mtb,[22-24] we sought to investigate the modulation of the autophagic process in human primary DC infected by Mtb and the vaccine strain BCG. We show that Mtb, but not BCG, impairs the late steps of autophagy and a functional ESX-1 secretion system is required for this inhibition. In addition, rapamycin treatment restored autophagy in Mtb-infected DC, which displayed an enhanced capacity to promote the expansion of Th1-oriented $CD4^+$ T cells. Collectively, these results highlight a unique cross-talk between Mtb and the autophagic process in DC, which could play a role in preventing an efficient antimycobacterial immune response.

Results

Mtb and BCG have different impacts on the autophagic process in human primary DC. To set up our experimental model, we faced an issue related to the use of IL4 and granulocyte-macrophage colony stimulating factor (CSF2) for the in vitro differentiation of monocyte-derived DC. Given the inhibitory effect exerted by IL4 on autophagy[25] and the activation of MTOR pathway by CSF2 and IL4 along monocyte-derived DC,[26] we compared in preliminary experiments the effect of Mtb infection on the autophagic process in the presence of CSF2 and IL4 or following the replacement of the differentiating medium 20 h before infection. Having found that both the basal and Mtb-driven autophagic response was altered by the presence of IL4 and CSF2 (data not shown), we decided to perform our study in DC starved from these differentiating cytokines.

Autophagy levels were analyzed in primary human DC infected with either Mtb or BCG at a multiplicity of infection (MOI) of 1. Cells were harvested 24 h after infection and the occurrence of autophagy was monitored by both immunoblotting and immunostaining using an antimicrotubule-associated protein 1 light chain 3 (MAP1LC3) antibody. As shown in **Figure 1A**, Mtb induced a significant increase of MAP1LC3-II, the processed isoform of MAP1LC3 associated with autophagosomes. This increase was accompanied by an accumulation of MAP1LC3-positive vesicles observed by confocal microscopy (**Fig. 1B**). Notably, MAP1LC3-II increase was not observed when cells were infected with either BCG or stimulated with heat-inactivated Mtb, suggesting that only live, virulent mycobacteria are able to modulate MAP1LC3-II levels (**Fig. 1A and B**). Autophagosome accumulation observed during Mtb infection was prevented by incubating DC with the autophagy inhibitor wortmannin, confirming the specificity of MAP1LC3-positive vescicles observed in Mtb-infected DC (**Fig. S1**).

We then asked whether the accumulation of MAP1LC3-II was an early or late event during Mtb infection. MAP1LC3 levels were analyzed in DC harvested by immunoblotting (**Fig. 1C**) and confocal microscopy (**Fig. 1D**) at different time points after Mtb infection. MAP1LC3 II increase occurs at late times, being slightly induced at 8 h and increasing at 16 h, although Mtb was already detected intracellularly at earlier times (**Fig. 1E**), as revealed by confocal microscopy performed with a Cherry-expressing Mtb following the visualization of DC plasma membrane using a FITC-conjugated DR antibody.

Mtb causes a block of autophagosome maturation. The accumulation of MAP1LC3-II in Mtb-infected cells could be due to an enhanced autophagosome formation or a reduced degradation of autophagic material.[17,25] To discriminate between these events, we assessed the occurrence of a functional autophagic flux in Mtb-infected cells. To this aim, we analyzed the lysosome-mediated autophagosome degradation by monitoring either the effect of lysosomal inhibitors on MAP1LC3 levels or the colocalization of autophagosomes with lysosomal markers. Both

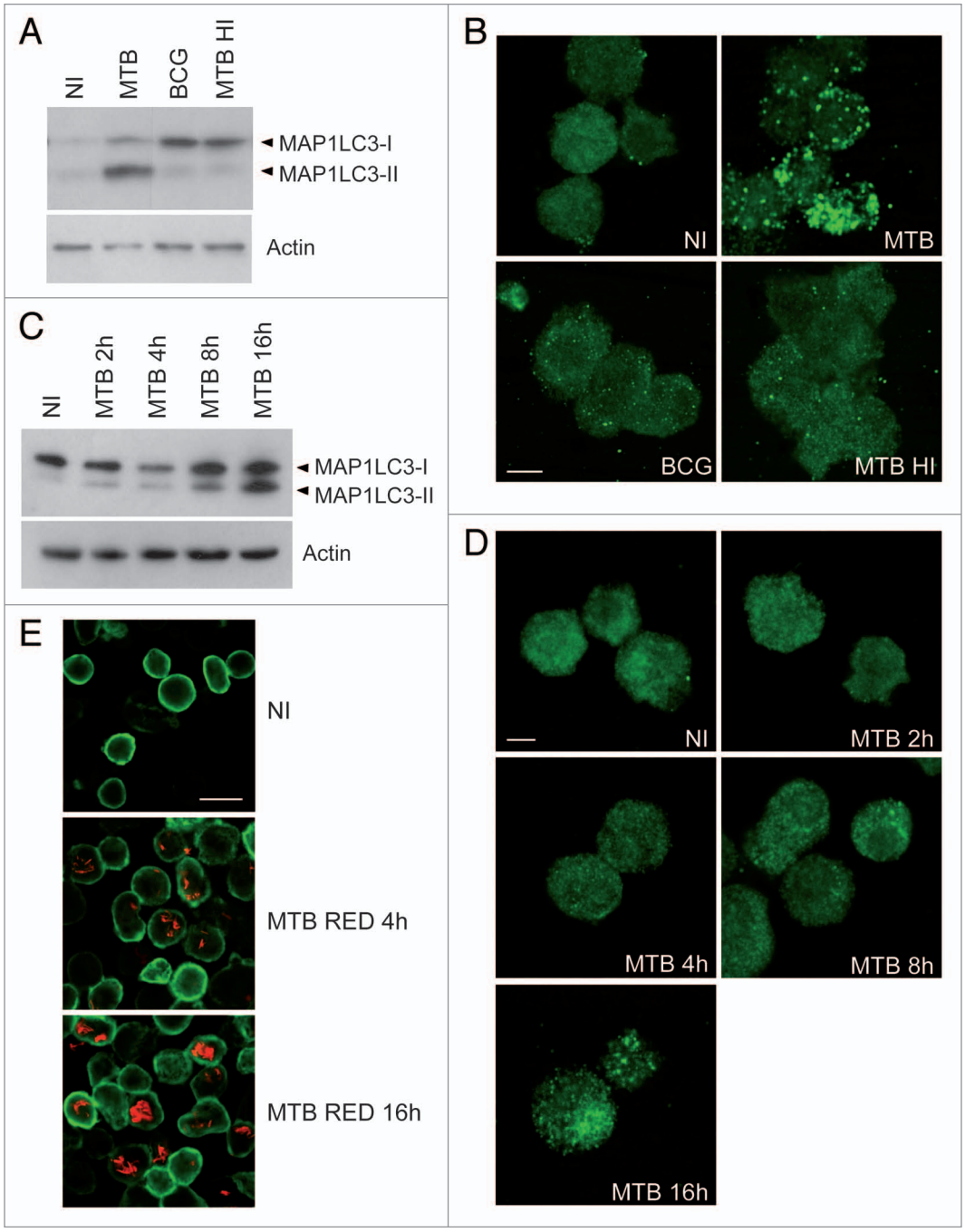

Figure 1. Modulation of autophagy by Mtb. (A and B) DC were infected with Mtb, BCG or heat-inactivated Mtb (Mtb HI). After 24 h, autophagy levels were analyzed for MAP1LC3 expression by immunoblotting (A) or immunofluorescence using an MAP1LC3 antibody (B). Scale bar: 6 μm. (C and D) DC were infected with Mtb. At the indicated time points after infection, cells were analyzed for either MAP1LC3 levels by immunoblotting (C) or by confocal microscopy (D). Scale bar: 6 μm. (E) DC were infected with a Cherry-expressing Mtb (Mtb RED). Four or 16 h after infection, cells were analyzed for Mtb internalization by confocal microscopy following plasma membrane visualization using a FITC-conjugated HLA-DR antibody. Scale bar: 20 μm. NI: not infected DC. Actin levels were analyzed to verify protein amount loading.

analyses indicated that autophagosome accumulation in Mtb-infected cells was due to a defect in the late steps of the autophagic process. As shown in **Figure 2A**, treatment of Mtb-infected DC with the lysosomal protease inhibitors E64d and Pepstatin A (PepA) resulted in a reduced increase of MAP1LC3-II protein levels [1.3 fold, calculated as the ratio between MAP1LC3 levels in Mtb-infected DC treated with E64D+PepA (6.4) and those in untreated Mtb-infected DC (5.1)] as compared with the effect promoted by the same treatment in not-infected cells (3.8 fold), suggesting that MAP1LC3-II degradation by lysosomal enzymes is impaired during Mtb infection. Similar results were obtained when the levels of SQSTM1 protein, a well-characterized target

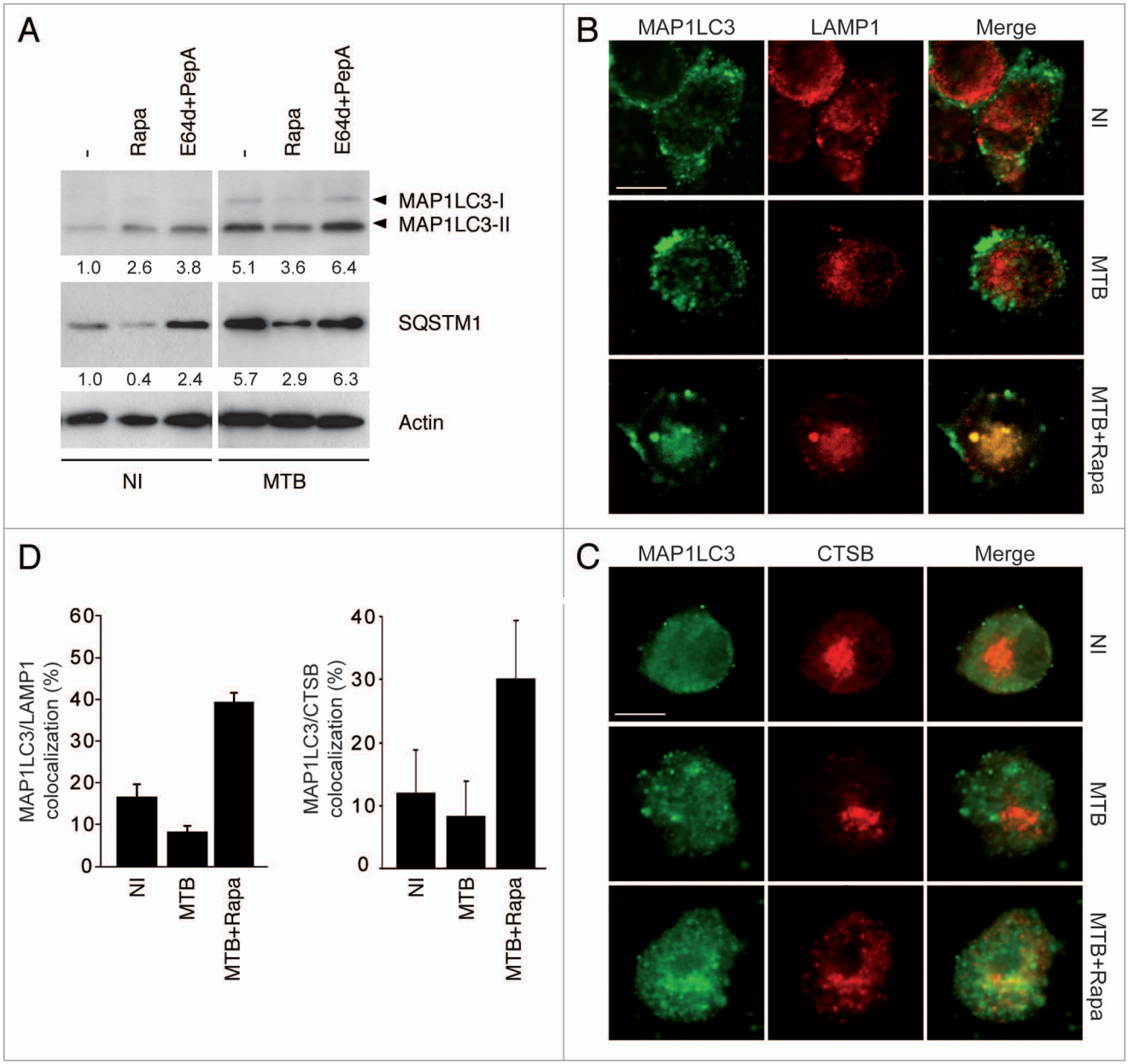

Figure 2. Effects of rapamycin on autophagic flux in Mtb-infectd DC. (A) DC were infected with Mtb and treated with rapamycin (Rapa, 0.2 μM; 4 h after infection) or E64d plus PepA A (E64d+PepA, 10 μg/ml each, 4 h before cell harvesting) or left untreated (vehicle, DMSO). Cells were harvested 24 h after infection and analyzed for MAP1LC3 and SQSTM1 levels by immunoblotting. Quantification of the MAP1LC3 and SQSTM1 levels was indicated at the bottom of each immunoblot. The results shown are from one of three experiments that yielded similar results. NI: not infected DC. Actin levels were analyzed to verify protein amount loading. (B and C) Immunofluorescence analysis of MAP1LC3 and LAMP1 (B) or CTSB (C) co-localization in Mtb-infected cells. Mtb-infected cells were incubated with rapamycin, as described in (A), or left untreated, fixed 24 h after infection and stained for MAP1LC3 and LAMP1 (B) and MAP1LC3 and CTSB (C). The images showing the merge of the two fluorescence signals (Red: LAMP1 and CTSB; Green: MAP1LC3) are shown on the right panels. Scale bar: 10 μm. (D) Graphics reporting a quantification of the experiments described in (B and C) performed as indicated in Materials and Methods. The results represent the mean ± standard error of the mean (SEM) of three independent experiments.

of the autophagic process, were analyzed in the same experimental setting. Indeed, Mtb infection leads to the accumulation of SQSTM1 protein (5.7 fold) which is not further increased by treatment with lysosomal inhibitors (1.1 fold), different from what was observed in control cells (2.4 fold, **Fig. 2A**). It should be pointed out that SQSTM1 increase in Mtb-infected DC is not only due to an impairment of protein degradation, since an induction at the transcriptional level was also observed during infection (2.5 fold induction, **Fig. S2A**). Similar results were obtained when lysosome activity in Mtb-infected DC was interfered using bafilomycin A_1, an inhibitor of the vacuolar-type H^+-ATPase (1.2 fold in Mtb-infected DC vs. 3.9 fold in not-infected cells, **Fig. S2B**). The impairment of autophagosome maturation was further investigated by confocal microscopy.

We observed a reduced colocalization between MAP1LC3 and the lysosomal markers lysosomal-associated membrane protein 1 (LAMP1) and cathepsin B (CTSB) in Mtb-infected cells (**Fig. 2B–D**), confirming that Mtb hampers the autophagic flux.

Rapamycin has been reported to promote autophagy-mediated clearance of Mtb in macrophages.[12] Thus, we decided to test whether rapamycin is able to overcome the impaired autophagic flux in Mtb-infected DC. Rapamycin was added 4 h after infection when the majority of cells showed the internalization of Mtb (see **Fig. 1E**). Western blot and confocal analyses showed that rapamycin treatment restores a functional autophagic flux as indicated by the reduction of SQSTM1 levels (**Fig. 2A**) as well as by the increased colocalization of MAP1LC3 with LAMP1 and CTSB, two markers of late endocytic/lysosomal compartments (**Fig. 2B–D**). Notably, rapamycin treatment led to a significant increase in Mtb-containing autophagosomes and autolysosomes, as evaluated by both electron and confocal microscopy (**Fig. 3**). Interestingly, confocal microscopy analysis showed not only an increased Mtb-MAP1LC3 colocalization following rapamycin treatment (**Fig. 3B and E**), but also a robust formation of Mtb-containing autolysosomes positive to LAMP1 (**Fig. 3C and E**). Mtb-MAP1LC3 colocalization induced by rapamycin is prevented by pretreating cells with wortmannin (**Fig. S2C**). To further characterize the intracellular Mtb localization after rapamycin treatment, the acidification of Mtb-containing phagosome was evaluated using LysoTracker, a fluorescent dye for labeling acidic organelles (**Fig. 3D and E**). Mtb was found within LysoTracker positive lysosome only after rapamycin treatment. Interestingly, the ability to rescue the inhibition of autophagic flux imposed by Mtb is not restricted to rapamycin, as it was also observed by treating cells with IFNG (**Fig. S3**), a known inducer of autophagosome formation.[12] Indeed, in IFNG stimulated DC Mtb localized with MAP1LC3 in LAMP1 positive compartment, likely autolysosome. Altogether these results indicate that, although a high number of autophagosomes accumulate in Mtb-infected DC, their maturation into the autolysosome is reached only after the treatment with autophagy inducers, such as rapamycin and IFNG.

ESX-1 is responsible for the inhibition of autophagosome maturation by Mtb. The different modulation of autophagy by Mtb and BCG prompted us to better characterize the mycobacterial factors responsible for this phenomenon. DC were infected with recombinant Mtb strains, which were deleted for either the entire RD1 region (MtbΔRD1::pYUB412),[27] or the promoter region of the CFP-10/ESAT-6 operon, preventing ESAT-6 and CFP-10 expression. Furthermore we tested a recombinant Mtb strain secreting an ESAT-6 variant lacking 12 aa of C-terminus (ESAT-6Δ84–95). These recombinant strains resulted attenuated in the TB mouse infection model.[28,29] Notably, all tested deletion mutants have lost the ability to accumulate MAP1LC3-II as well as to prevent MAP1LC3/LAMP1 colocalization (**Fig. 4A–C**), thus indicating that secretion of biologically functional ESAT-6/CFP-10 is a requirement for the inhibition of autophagosome maturation by Mtb.

In order to better elucidate the functional relationship between the RD1 encoded ESX-1 secretion system and the autophagic process, we decided to test the modulation of autophagy in DC infected with BCG complemented with a 32 kb fragment from Mtb spanning the extended RD1 region (BCG::RD1),[30] which actively secretes ESAT-6 and CFP-10. Cells infected with the BCG::RD1 strain depicted an accumulation of MAP1LC3-II protein similar to what was observed for Mtb (**Fig. 4D**). Finally, we tested the attenuated Mtb H37Ra strain, which shows an impaired secretion of ESAT-6 due to a point mutation in the DNA-binding region of the regulator PhoP. We analyzed the effect on autophagy of Mtb H37Ra and recombinant H37Ra strain complemented with a wild-type copy of *phoP* (Rv0757), which has been described to restore the ability of the H37Ra (H37Ra::PhoP) to secrete ESAT-6 and to elicit specific T-cell responses,[31] in comparison with a strain complemented with an unrelated gene (H37Ra::RpsL). Strikingly, infection of DC with H37Ra::PhoP promoted MAP1LC3-II accumulation (**Fig. 4D**), whereas this effect was not observed with the Mtb H37Ra and H37Ra::RpsL strains. Taken together, these findings indicate that mycobacterial inhibition of autophagy in DC is dependent on the ability of mycobacteria strains to secrete intact ESAT-6/CFP-10.

Rapamycin enhances the capacity of Mtb-infected DC to promote a Th1-oriented response. Having found that rapamycin treatment overcomes the block in autophagosome maturation by Mtb, we sought to investigate the impact of this reversion on DC function. Initially, we evaluated whether rapamycin could modulate Mtb-induced DC maturation. Previous findings showed that rapamycin suppressed immunostimulatory molecules and the allostimulatory potential of LPS-stimulated DC.[26] However, when we investigated by flow cytometry analysis the immunophenotype of DC, no major differences were observed on the Mtb-induced expression of the molecules involved in T cell activation, such as CD86, CD83, HLA-DR and CD38 (**Table 1**). Also, no modulation of Mtb-induced tumor necrosis factor (TNF) production was observed upon rapamycin treatment (**Fig. 5A**). Conversely, the expression of cytokines involved in the polarization of Th1 lymphocytes was enhanced in Mtb-infected DC cultures upon rapamycin addition (**Fig. 5B and C**), namely interleukin (IL)12 p70 and interferon (IFN)B1. In particular, a significant induction of Mtb-stimulated production of interleukin (IL)12 p70 was observed following rapamycin treatment, (**Fig. 5B**). A similar result was obtained by studying interferon (IFN)B1 expression performed by real-time RT-PCR (**Fig. 5C**). Indeed, the induction of IFNB1 mRNA observed in Mtb-infected DC was further enhanced after exposure to rapamycin, although this increase was not statistically significant. Interestingly, also the treatment with another autophagy inducer, IFNG, enhances the IL12 production in Mtb-infected cultures (**Fig. S4A**), suggesting that the expression of this Th1 promoting cytokine could be linked to the autophagic process. In line with this result, E64D and PepA treatment abolishes Mtb-induced IL12 expression, while exerts a limited effect on TNF release (**Fig. S4B**).

To evaluate whether the effect induced by rapamycin on the secretion of Th1 cytokines from Mtb-stimulated DC resulted in an enhanced capacity to expand a Th1-oriented $CD4^+$ T cell

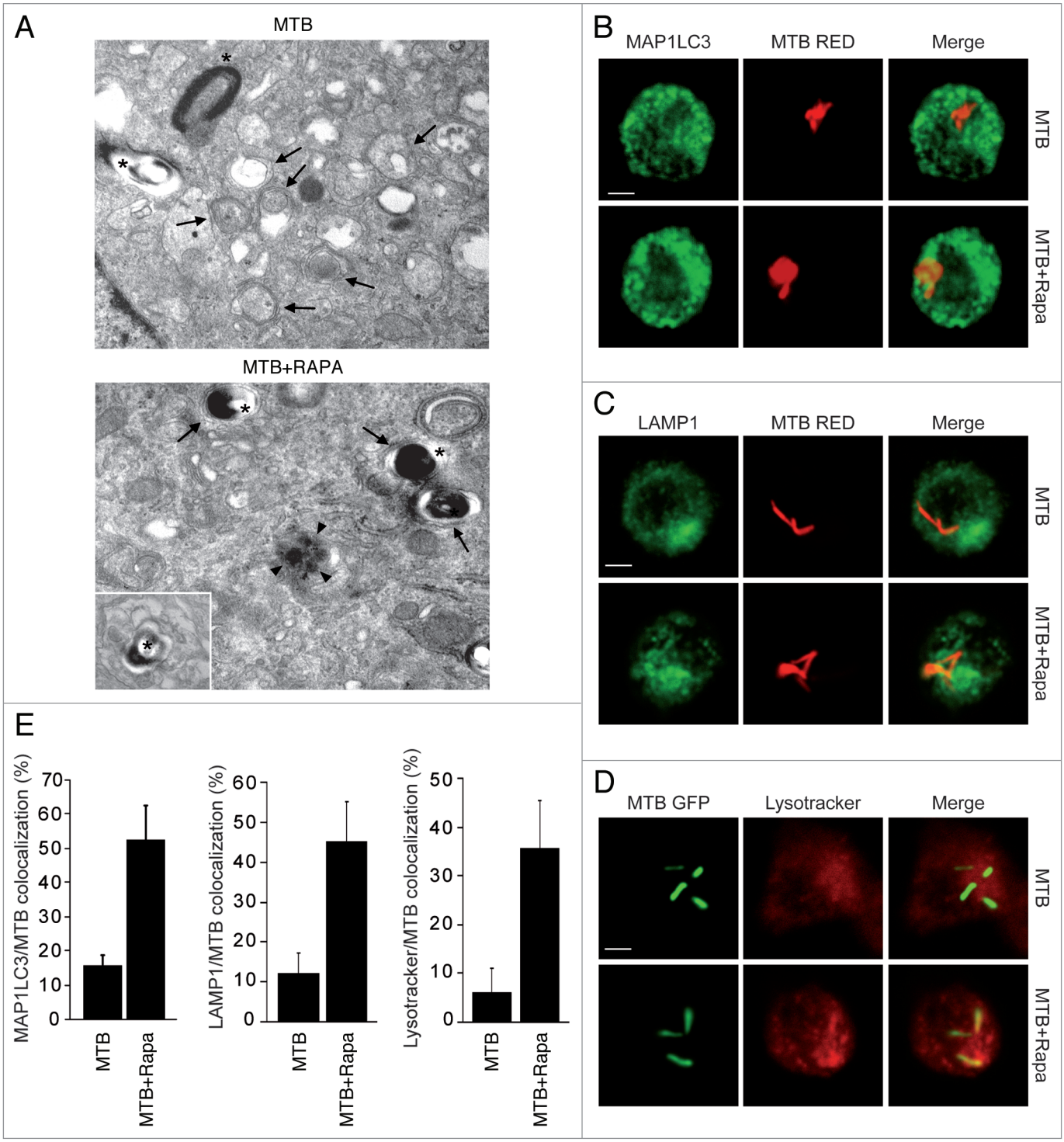

Figure 3. Inhibition of autophagosome maturation by Mtb (A) Ultrastructural analysis of Mtb-infected DC 24 h post-infection either untreated (upper panel) or incubated with rapamycin (bottom panel) as described in **Figure 2A**. Autophagic vesicles, characterized by the presence of double membranes, are indicated by arrows in DC. Autolysosomes in which remnants of degraded cytoplasmic materials are indicated by arrowheads. Mycobacteria are indicated by asterisks (*). A partially digested bacterium inside a late autophagic vacuole is shown in the insert. Original magnification: 20.000x. (B and C) Mtb RED-infected cells were incubated with rapamycin, as described in **Figure 2A**, or left untreated, fixed 24 h after infection and stained for MAP1LC3 (B) or LAMP1 (C). The images showing the merge of the two fluorescence signals (Red: Mtb; Green: MAP1LC3 or LAMP1) are shown on the right panels. Scale bar: 5 μm. (D) DC were infected with Mtb GFP and treated with rapamycin, as described in **Figure 2A**, or left untreated. Twenty-four hours after infection, DC were incubated with LysoTracker (500 nM) for 30 min and then fixed in 4% PAF. The images showing the merge of the two fluorescence signals (Red: LysoTracker; Green: Mtb) are shown on the right panels. Scale bar: 5 μm. (E) Graphics reporting a quantification of the experiments described in (B–D) performed as indicated in Materials and Methods. The results represent the mean ± SEM of three independent experiments.

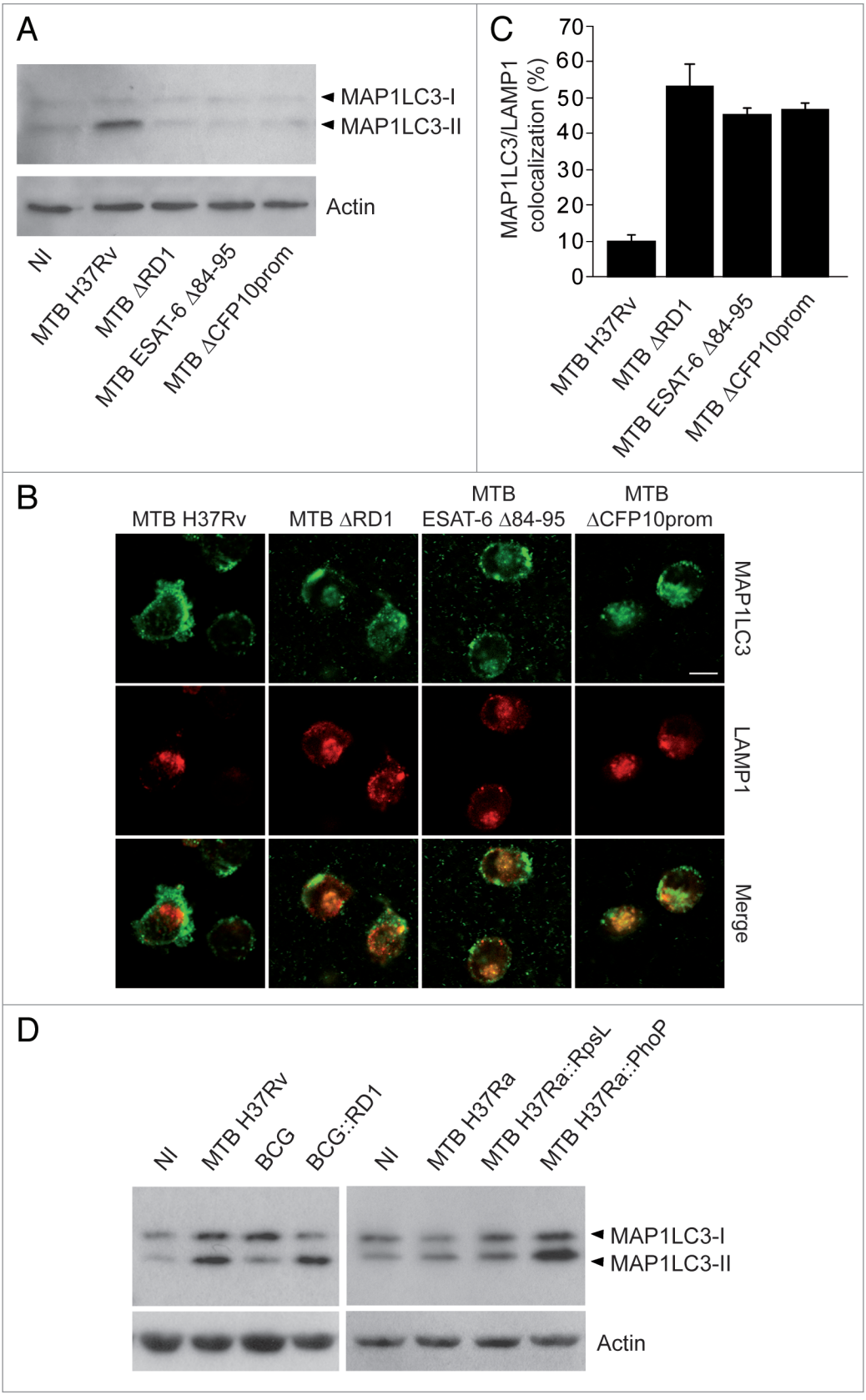

Figure 4. For figure legend, see page 1364.

Figure 4 (See previous page). Autophagy inhibition by ESX1/type VII secretion system. (A) DC were infected with wild-type Mtb (H37Rv) or with the following Mtb strains: H37RvΔRD1::empty vector pYUB412, H37RvΔRD1::RD1–2F9-ESAT-6-Δ84–95, H37RvΔRD1::RD1–2F9ΔCFP-10prom. Cells were harvested 24 h after infection and analyzed for LC3 levels by immunoblotting. (B) Immunofluorescence analysis of MAP1LC3 and LAMP1 colocalization was performed in cells infected with wild-type Mtb or the indicated mutant strains. DC were fixed 24 h after infection and stained for MAP1LC3 and LAMP1. The images displaying the merge of the two fluorescence signals (Red: LAMP1; Green: MAP1LC3) are shown on the bottom panels. Scale bar: 10 μ.m. (C) Graphics reporting a quantification of the experiments described in (B) performed as indicated in Materials and Methods. The results represent the mean ± SEM of three independent experiments. (D) DC were infected with Mtb H37Rv, BCG, BCG::RD1, H37Ra, H37Ra::RpsL and H37Ra::PhoP strains. Cells were harvested 24 h after infection and analyzed for MAP1LC3 levels by immunoblotting. Actin levels were analyzed to verify protein amount loading. NI: not infected DC.

Table 1. Rapamycin effect on the expression of maturation markers in DC infected with Mtb

	CD86	CD38	HLA-DR	CD83
NI[a]	22.3 ± 15.3[b]	5.7 ± 2.3	83 ± 22	8 ± 4
Rapa	13 ± 7	6.3 ± 0.9	56.3 ± 22	9 ± 3
Mtb	109 ± 26	15.3 ± 4.4	121 ± 13	18 ± 3
Mtb+Rapa	98.3 ± 28	17.3 ± 6	132 ± 26	20 ± 5

[a]NI: not infected DC. [b]The expression of the cell-surface molecules was evaluated using the mean fluorescence intensity (MFI) after subtraction of the values of the isotype controls. Values are reported as MFI ± SEM measured in three independent experiments.

population, we studied T-cell polarization by mixed lymphocyte reaction (MLR) experiments. As shown in **Figure 5D**, the rapamycin treatment enhanced the production of IFNG. IL12 neutralization with specific monoclonal antibodies drastically reduced IFNG levels in co-cultures with DC infected with Mtb both in presence or absence of rapamycin, suggesting that the enhanced expression of IL12 induced by rapamycin may represent a key event for the expansion of an anti-Mtb Th1 response mediated by DC. No induction of IL4 and IL5 was observed when T cells were co-cultured for 5 d with Mtb-stimulated DC in the presence or absence of rapamycin (data not shown).

Finally, we evaluated the autophagy-mediated killing of the tubercle bacilli by CFU assay (**Fig. S5**). A bacteriostatic effect on mycobacterial growth rather than a reduction in Mtb viability was observed upon rapamycin treatment at 3 d, pointing at a major role of autophagy in DC in the induction of an efficient T cell response rather than Mtb killing, a function mainly exerted by macrophages.[13]

Collectively, these results provide evidence of the capacity of rapamycin to promote Mtb-infected DC to stimulate a Th1 response likely by overcoming the mycobacterial phagosome maturation block and enhancing IL12 production.

Discussion

In light of the importance of the autophagic process in different facets of antigen presentation,[32] there is an increasing interest in exploiting this pathway for optimizing Mtb vaccine strategies. For this reason, particular attention is currently devoted to the role of autophagy in DC, which represent key effectors of the immune response against Mtb.[22,23,33] At variance with macrophages, which are primarily involved in the containment of Mtb growth, DC are engaged in inducing a protective T cell response. A recent study in mouse DC indicated that both secreted Ag85B antigen and intact mycobacteria can be targeted into lysosomes for peptide production through autophagy.[13] These authors provided also the first in vivo evidence on the effects promoted by rapamycin in mouse DC infected with attenuated vaccine candidates. The rapamycin-mediated increase of Mtb antigen presentation occurring in DC, resulted in a strong expansion of a Th1 population in the spleen, in the improvement of Mtb clearance and in in vivo protection against virulent Mtb, generating a novel proof of principle that the efficacy of anti-TB vaccines can be enhanced through the modulation of autophagy. In line with these findings, autophagy is currently investigated as novel therapeutic target for preventing acquisition or reactivation of latent TB or to treat multidrug resistence and extensively-drug resistant TB.[34]

To extend this study to human primary DC, we investigated the autophagic process in DC infected with virulent or avirulent Mtb as well as the vaccine BCG strain. We found that Mtb promotes a significant increase of MAP1LC3-II level and an accumulation of autophagosomes, that was specific for the virulent strain since it was not observed during BCG or avirulent Mtb H37Ra infection, or stimulation with heat-inactivated Mtb. The increased levels of autophagosomes in Mtb-infected DC was determined by a defective autophagic flux likely due to an impaired ability of autophagosomes to fuse with lysosomes, as shown by the reduced localization of MAP1LC3 with the lysosomal markers LAMP1 and cathepsin B, as well as by the impaired lysosomal degradation activity, assessed by comparing MAP1LC3-II and SQSTM1 levels in the presence or absence of lysosome inhibitors, such as E64D plus PepA or bafilomycin A_1.

No differences have been outlined so far on the capacity of these mycobacterial strains to modulate the autophagic process. This is possibly due to the fact that previous studies were mainly performed on cell lines rather than primary cultures, and they were focused on the effect of autophagy induced by cytokines or pharmacological agents rather than on the modulation of basal autophagy.[12] We believe that our results provide an important indication for future studies, underlining that the use of attenuated strains such as BCG or Mtb H37Ra in the study of the interaction of Mtb with the host immune system might not reflect what is occurring with fully virulent strains.

In the attempt to identify the molecular basis underlying autophagy inhibition in Mtb-infected DC, we investigated a variety of attenuated Mtb strains that were either lacking the major part of the ESX-1 secretion system, the promoter region of the CFP-10/ESAT-6 operon, or the C-terminus of the secreted effector protein ESAT-6. We also studied a variant of the attenuated Mtb H37Ra strain, which regained the ability of secreting ESAT-6 and CFP-10

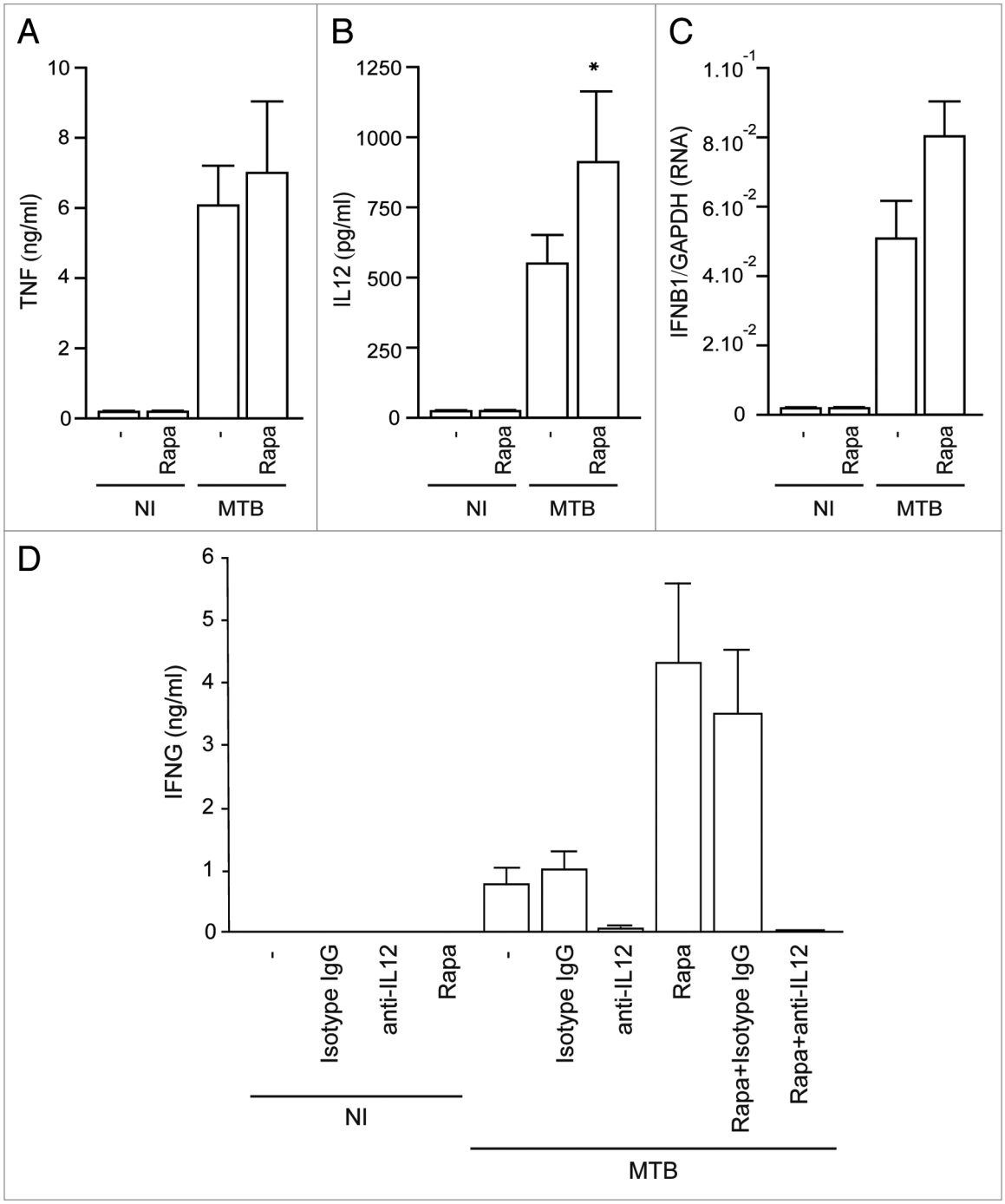

Figure 5. Effect of rapamycin on DC maturation. (A and B) Cell culture supernatants were collected from DC cultures infected with Mtb and treated with rapamycin as in Figure 2A, or left untreated. The production of TNF (A) IL12 (B) was measured by CBA Flex Set. The results represent the mean ± SEM of seven independent experiments. (*p = 0.018 Mtb vs. Mtb+Rapa). (C) Real-time RT-PCR was performed to measure the expression of IFNB1 transcripts. The results shown are from one out three experiments performed with different donors that yielded similar results. Levels of IFNB1 mRNA are normalized to the GAPDH level using the Equation $2^{-\Delta Ct}$; the values shown are means ± SD of triplicate determinations. (D) The response of allogeneic naïve $CD4^+$ T cells upon co-culture with Mtb-infected DC in presence or absence of treatment with rapamycin was evaluated by MLR. Where indicated the production of IL12 was neutralized by the addition of neutralizing monoclonal anti IL12 antibody. Allogeneic naïve $CD4^+$ T were cultured with DC at 1:10 ratio (stimulator:effector cell) for 5 d and the levels of cytokines were evaluated by CBA Flex set. The results shown represent the mean ± SEM of three independent experiments. NI: not infected DC.

by complementation with the phoP regulator from Mtb H37Rv. Both approaches showed that impairment of the autophagic flux only occurred if the engulfed live mycobacteria had the capacity to secrete intact ESAT-6/CFP-10 via the ESX-1/type VII secretion system. In line with these results, our data obtained with heat killed Mtb (**Fig. 1A**) showed that the interaction and the

internalization of the bacteria inside DC are not yet sufficient for the inhibition of autophagy since the accumulation of the membrane-bound form MAP1LC3-II was observed when production and secretion of different Mtb effector proteins is likely to occur.

How the ESX-1 system could negatively regulate the autophagic process remains to be elucidated. The lack of ESAT-6 or CFP-10 antibodies functioning in intracellular detection assays prevented us to verify whether these proteins localize with autophagosomes. However, it is important to underline that also the truncated form of ESAT-6 lacking 12 residues at C-terminus seems to be unable to affect the autophagic flux since no MAP1LC3-II accumulation was observed. As the extreme C terminus of ESAT-6 represents a floppy, structurally not well-defined region of the protein,[35] it is likely that this region is free to interact with host proteins or might help the interaction of ESAT-6 with the lipid bilayers of the subcellular organelles or the cell membrane.[27,36] As an alternative to a direct interaction of ESAT-6 with the autophagic machinery, ESX-1 proteins could allow other Mtb-encoded factors to translocate into the cytosol to inhibit the autophagy flux. In this regard, a potential candidate for the antiautophagic activity of Mtb could be the phosphatidylinositol 3-phosphate phosphatase SapM, which has been described to block BCG-containing phagosome maturation.[37] Interestingly, a recent observation by Shin and collaborators[38] showed that the Mtb enhanced intracellular survival (Eis) factor, which is also released in the cytoplasm of infected macrophages,[39] negatively regulates autophagy induction in murine macrophages. Although the specific contribution of Eis in infected DC remains to be characterized, these results suggest that Mtb could have adopted different strategies to interfere with distinct steps of autophagy.

It has also been reported that ESX-1 is required for the translocation of *M. marinum* and/or Mtb to the host cell cytosol.[40-44] However, since Mtb is still detected in vesicle structures 16 h after infection (ref. 44 and data not shown) when autophagy block is already fully visible, it is likely that the effect on autophagy was not exerted by cytosolic Mtb. In this context, it is conceivable that the membrane-lysing or pore-forming activity exerted by ESAT-6 and/or other effector proteins of the ESX-1 system might be responsible for autophagy blockage during the early phases of infection while at later stages it allows the phagosome-to-cytosol translocation of Mtb.[40-44] Although in our experimental model it is not yet clear whether ESAT-6 modulates directly or indirectly the autophagic process, the results obtained so far strongly suggest that the functional interaction between ESAT-6 and the DC autophagosome/autolysosome machinery is crucial to influence the immune response against TB.[30]

We also showed that rapamycin treatment restores a functional autophagic flux in Mtb-infected cells, as evaluated by the analysis of SQSTM1 levels and the colocalization of MAP1LC3 with the lysosomal markers LAMP1 and cathepsin B. These results also showed that, although a high number of autophagosomes are present in infected DC, autophagy does not target Mtb for lysosome degradation unless cells are treated with rapamycin, an effect that was prevented by the simultaneous addition of the conventional inhibitor of autophagy, wortmannin.

Since rapamycin is known to induce autophagy by inhibiting the activity of MTOR, an upstream negative regulator of this process, it is plausible that the effect of rapamycin is due to a rise of the levels of autophagy above a threshold, which cannot be further blocked by Mtb. In addition, we observed that IFNG has positive effects on autophagy similar to rapamycin, as shown previously by Gutierrez and colleagues.[12] Indeed, activation of Mtb-infected DC with IFNG resulted in an enhanced degradation of SQSTM1 level and increased colocalization of Mtb with MAP1LC3 and LAMP1.

To provide functional relevance to these observations, we investigated the effect of rapamycin on autophagy-mediated killing of the tubercle bacilli and on Mtb-induced DC maturation. Rapamycin induced a bacteriostatic effect on mycobacterial growth rather than a reduction in Mtb viability, which conversely occurs in Mtb-infected macrophages.[14] Moreover, while no significant differences were detected in the level of maturation markers in Mtb-infected DC upon rapamycin treatment, we observed a statistically significant enhancement of IL12 production. In addition, the secretion of IL12 in Mtb-infected cells was also promoted by IFNG, confirming the existence of a link between the intracellular pathways regulating autophagy process and the release of this Th1 promoting cytokine in DC. Accordingly, treatment of infected DC with E64D plus PepA abolishes Mtb-mediated induction of IL12, irrespective to the presence of rapamycin or IFNG, indicating that lysosomal activity is required for essential events of DC maturation process, such as the release of IL12, a crucial Th1 promoting cytokine. Moreover, an increased expression of IFNB1 was also evidentiated in Mtb-infected DC upon rapamycin treatment, which likely synergizes with IL12 in promoting a Th1 response as previously described.[34] In this scenario it is likely that the expansion of IFNG producing cells may potentiate the autophagic processes in DC as well as in macrophages,[15,16,45] which represent crucial regulators of both innate and adaptive immune response against pathogens, including intracellular mycobacteria.[22,23] Although the involvement of components of autophagic machinery in the production of inflammatory cytokines in response to endotoxin or viral infections has been reported,[46-48] no data are available so far on the regulation of cytokine expression by autophagy in Mtb-infected cells. Therefore, it would be important to identify the molecular mechanisms underlying the enhancement of IL12 and IFNB1 expression by rapamycin and IFNG in Mtb-infected DC in order to improve their immunoregulatory properties.

Collectively, our results shed light on novel aspect of DC-Mtb interaction, which could offer a new target for vaccine design and adjunctive immunotherapy with autophagy-promoting agents for the improvement of TB control.

Material and Methods

Antibodies and other reagents. Monoclonal antibodies (BD Bioscience) specific for CD1a (555806), CD14 (555398), CD38 (555460), CD86 (555657), HLA-DR (555811), CD83 (556855), IgG1 (555748), IgG2a (553457) were used as direct conjugates

to FITC (Fluorescein Isothiocyanate) or PE (Phycoerythrin). Rabbit anti-MAP1LC3 for immunoblotting analysis (Cell Signaling, 2775), rabbit anti-MAP1LC3 for confocal microscopy (Sigma-Aldrich, L7543), mouse anti-LAMP1 (Abcam, ab25630), mouse anti-actin (Sigma-Aldrich, A2066), mouse anti-SQSTM1 (SQSTM1 D3, Santa Cruz Biotechnology, sc28359), mouse anti-cathepsin B (Calbiochem, IM27L). For autophagy induction, rapamycin (0.2 μM; Sigma-Aldrich, R0395) or with 10 ng/ml of IFNG (Pepro Tech EC LTD, 300-02) was added to DC cultures. To inhibit lysosomal activity, cells were incubated with 10 μg/ml E64d (Sigma-Aldrich, E8460) together with 10 μg/ml PepA (Sigma-Aldrich, P5318), bafilomycin A_1 (Sigma-Aldrich, B1793), while wortmannin 1 μM (Sigma-Aldrich, W1628) was used as a pharmacological inhibitor of autophagy. The optimal concentration of rapamycin and E64d plus PepA was evaluated in preliminary dose-response experiments, while the treatment time is specified in each figure legend.

DC preparation. DC were prepared as previously described.[49] Briefly, peripheral blood mononuclear cells were isolated from freshly collected buffy coats obtained from healthy voluntary blood donors (Blood Bank of University "La Sapienza," Rome, Italy) by density gradient centrifugation using Lympholyte-H (Cedarlane, CL 5020). Monocytes were purified by positive sorting using anti-CD14 conjugated magnetic microbeads (Miltenyi, 130-050-201). The recovered cells were > 99% $CD14^+$ as determined by flow cytometry with anti-CD14 antibody. DC were generated by culturing monocytes in 6-well tissue culture plates (Costar Corporation, 3516) with 50 ng/ml CSF2 (R&D Systems, 215-GM) and 1000 U/ml of IL4 (R&D Systems, 204-IL) for 5 d at 0.5 × 10^6 cells/ml in RPMI 1640 (BioWhittaker, BE12-167F) supplemented with 2 mM L-glutamine (BioWhittaker, BE17-605E) and 15% FCS (BioWhittaker, DE14-801F). No antibiotics were added to the cultures. At day 5 the cells were 90% $CD1a^+$ and 95% $CD14^-$. The differentiation medium containing IL4 and CSF2 was removed and replaced with RPMI supplemented with 2 mM L-glutamine and 15% FCS before Mtb infection to avoid cytokine-driven modulation of the autophagic and MTOR pathway.

Bacteria preparation and infection of DC. Mtb H37Rv (ATCC 27294; American Type Culture Collection) and M. *bovis* BCG (ATCC 27291) were used to infect DC cultures. As regards the recombinant strains used in this study, they were derived from Mtb H37RvΔRD1[27] or BCG Pasteur (1173P2) by integrating either the empty vector pYUB412, or pRD1-2F9 that carries a 32 kb fragment from Mtb H37Rv overlapping the extended RD1 region, or modified versions of pRD1-2F9 deleted for the promoter region of the CFP-10/ESAT-6 operon (ΔCFP-10prom) or the 11 C-terminal codons of ESAT-6 (ESAT-6-Δ84-95).[28,29] Mtb H37Ra, the recombinant strain H37Ra::PhoP containing the wild-type PhoP gene and the strain complemented with an unrelated gene (H37Ra::RpsL) were previously described in Frigui et al.[31] The plasmid pSMT3-DsRed (kindly by Wilbert Bitter, VU University, Amsterdam), and containing a cassette with the gene encoding the red fluorescent protein cherry under the control of the hsp60 promoter, was electroporated in Mtb H37Rv following standard procedures.[50] The cloning of the recombinant Mtb H37Rv GFP was previously described by Delogu and collaborators.[51] Recombinant Mtb H37Rv Ds-Red *cherry* as well as Mtb H37Rv GFP were cultured on 7H11 agar (BD Bioscience, 283810) supplemented with OADC (BD Bioscience, 211886) and with 50 μg/ml of hygromycin (Sigma-Aldrich, H9773) or in 7H9 liquid medium (BD Bioscience, 271310) supplemented with ADC (BD Bioscience, 211887), glycerol (Sigma-Aldrich, G5516) (0.5% vol/vol), 0.05% Tween 80 (Sigma-Aldrich, P1754), and containing 50 μg/ml of hygromycin until late log phase. One-ml of culture aliquots containing 10% of glycerol were stored at -80°C until use.

Mycobacteria were grown with gentle agitation (80 rpm) in 7H9 liquid medium supplemented with 0.05% Tween 80 and 10% OADC. Logarithmically growing cultures were centrifuged at 800 rpm for 10 min to eliminate clumped mycobacteria and then washed three times in RPMI 1640. Mycobacteria were resuspended in RPMI 1640 containing 10% FCS and then stored at -80°C. Vials were thawed and bacterial viability was determined by counting the number of colony forming units (CFU) on Middlebrook 7H10 agar plates (BD Bioscience, 262710). All bacteria preparations were analyzed for LPS contamination by the Limulus lysate assay (BioWhittaker, 50-647U) and contained less than 1 EU/ml. DC cultures were infected with a MOI of 1 bacteria/cell. Where indicated, Mtb was heat killed at 80°C for 1 h.

CFU assay. Four h after infection, the cell cultures were gently washed (three times) with RPMI 1640. DC were centrifuged at 150 × g for 10 min to selectively spin down cells while extracellular bacteria remain in the supernatants. Cells (~300.000) were resuspended in complete medium and cultured for the times indicated. Triplicate samples were assayed for CFU. At each time point cells were lysed with water containing 0.05% saponin (Sigma-Aldrich, 84510). Serial dilutions of the bacterial suspensions were plated (in duplicate) on 7H10 agar plates and viable bacteria were evaluated after 3 weeks of incubation at 37°C. Values are expressed as CFU/well.

Flow cytometry analysis. Approximately 1–2 × 10^5 cells were aliquoted into tubes and washed once in PBS containing 2% FCS. The cells were incubated with indicated antibodies (BD Bioscience) at 4°C for 30 min. The DC were then washed and fixed overnight with 4% paraformaldehyde (Pro-Labo, 20909290) before analysis on a FACSCan using CellQuest software (BD Bioscience).

Cytokine determination. Supernatants from DC cultures infected with Mtb and treated with rapamycin (0.2 μM) or E64d/PepA (10 μg/ml each) were harvested at 24 h after infection, filtered (0.2 μm) and stored at -80°C. The production of TNF (A) and IL12 (B) was measured by CBA Flex Set (BD Bioscience, 558472 for TNF, 558459 for IL12p70). The production of cytokines in MLR experiments was measured with human Th1/Th2 CBA Flex Set (BD Bioscience).

RNA isolation and real-time PCR quantifications. RNA was extracted from DC with RNeasy kit (Qiagen Inc., 74104) according to the manufacturer's instructions. A phenol/chloroform extraction was performed to inactivate residual mycobacterial particles. Reverse transcriptions and quantitative PCR assays were performed as previously described.[49] Primer pairs have been previously described.[49] The primers used for IFNB1

and GAPDH were previously described[33] while the oligonucleotides for SQSTM1 mRNA quantification were: 5'-ACA GAT GCC AGA ATC CGA AG-3' (forward) and 5'-TGG GAG AGG GAC TCA ATC AG-3' (reverse). Levels of IFNB1 and SQSTM1 mRNA are normalized to the GAPDH level using the Equation $2^{-\Delta Ct}$; the values are means ± SD of triplicate determinations

Immunoblotting analysis. Proteins were separated on 12% NuPAGE Bis-Tris gel (Invitrogen, NP0341) and electroblotted onto polyvinylidene fluoride membranes (Millipore, IPVH20200). Blots were incubated with primary antibodies in 5% nonfat dry milk in TBS plus 0.1% Tween20 (Sigma-Aldrich, P1379) overnight at 4°C. Detection was achieved using horseradish peroxidase-conjugate secondary antibody anti-mouse (Jackson Immunoresearch, 711-035-152), anti-rabbit (Jackson Immunoresearch, 715-035-150) and anti-goat (Jackson Immunoresearch, 705-035-147) and visualized with Enhanced Chemiluminescence plus (GE Healthcare, RPN2132). MAP1LC3-II/actin and SQSTM1/actin ratios were quantified by densitometric analysis using the ImageQuant software according to Rubinsztein et al.[52]

Confocal microscopy. Cells were fixed with 4% paraformaldehyde (Sigma-Aldrich, P6148) in PBS followed by permeabilization with 0.1% triton X-100 (Sigma-Aldrich, 93443) in PBS. Primary antibodies were incubated for 1 h at room temperature and visualized by means of Cy2-conjugated secondary antibodies (Jackson Immunoresearch, 711-226-152) and Cy3-conjugated secondary antibodies (Jackson Immunoresearch, 715-166-150). Coverslips were mounted in SlowFade-Anti-Fade (Invitrogen, S36939) and examined under a confocal microscope (Leica TCS SP2). For lysosome staining 500 nM Lysotracker Red (Invitrogen, L7528) was added to cells 30 min before fixation. Digital images were acquired with Leica software, and processed and quantified with ImageJ (National Institutes of Health) using a set of defined intensity thresholds that were applied to all images. A minimum of 50 cells per sample was counted for triplicate samples per condition in each experiment.

Transmission electron microscopy. DC cultures were analyzed 24 h after infection. Cells cultured in different conditions were fixed with 2.5% glutaraldehyde (Assin Spa, R1012) in 0.1 M cacodylate buffer for 1 h at 4°C (sodium cacodylate trihydrate, Sigma-Aldrich, C4945), and postfixed in 1% osmium tetroxide (Sigma-Aldrich, 75632) in 0.1 M cacodylate buffer for 1 h. The cells were then dehydrated in graded ethanol and embedded in Epon resin (AGAR 100, Agar Scientific R1045). Ultrathin sections were stained with 2% uranyl acetate (Sigma-Aldrich, 73943) and observed under a Zeiss EM900 transmission electron microscope. Images were captured digitally with a Mega View II digital camera (SIS; Zeiss).

MLR experiment. MLR was conducted as previously described.[49] $CD4^+$ T cells were purified from cord blood cells obtained from healthy voluntary donors (Cord Blood Bank of UOC Transfusion Medicine, S. Eugenio Hospital-ASL Roma C, Rome, Italy) by indirect magnetic sorting with a $CD4^+$ T-cell isolation kit (Miltenyi, 130-091-155). DC were infected with Mtb and 4 h after the infection rapamycin was added for additional 20 h. Immature DC, Mtb-infected DC with or without a rapamycin treatment were resuspended in 5% human AB serum (Euroclone, ECS0219D) complete medium prior to co-culture with naïve allogeneic cord blood $CD4^+$ T cells. Where indicated, neutralizing mouse monoclonal anti-IL12 antibody (R&D Systems, AB-219-NA) and its isotype control antibody (R&D Systems, MAB002) were added to DC/$CD4^+$ T cell co-culture at 20 μg/ml to neutralize the IL12. Supernatants from T cell/DC co-culture (ratio 10:1) were harvested at day 5 and analyzed for IFNG (560111), IL4 (558462) and IL5 (558463) release by CBA Flex set (BD Bioscience).

Ethics statement. Human blood was collected at the Blood Bank of University "La Sapienza" (Rome, Italy) and the Cord Blood Bank of UOC Transfusion Medicine, S. Eugenio Hospital (Rome, Italy) from healthy volunteers after written informed consent. Both blood centers operate under license from the Italian Ministry of Health. Therefore, the use of blood from these sources is exempt from our institutional review board.

Statistical analysis. Statistical analysis was calculated using a two-tailed for paired-data Student's t-test. A p value < 0.05 was considered statistically significant.

Disclosure of Potential Conflicts of Interest

No potential conflicts of interest were disclosed.

Acknowledgments

The study was supported by grants from Ministry for Health of Italy: "Ricerca Corrente" to M.P. G.M.F. and D.G.; "Ricerca Finalizzata" RF06.76.1, RF-IMI-2009-1302952 to D.G.; RF07.103 to E.M.C., G.M.F. and D.G.; by grants from the FP7 program of the European Community n°241745 to R.B. and E.M.C., n°40H58 to D.G. and APO-SYS Health F4-2007-200767 to M.P. The funders had no role in study design, data collection and analysis, decision to publish, or preparation of the manuscript.

The authors wish to thank Marco Tilotta and Tiziana Vescovo for the help provided in some of the experimental settings. We are deeply grateful to Blood Bank of University "La Sapienza" (Rome, Italy) and UOC Transfusion Medicine, S. Eugenio Hospital-ASL Roma C (Rome, Italy) for providing us with blood donations.

Supplemental Materials

Supplemental materials may be found here:
www.landesbioscience.com/journals/autophagy/article/20881

References

1. Liu J, Tran V, Leung AS, Alexander DC, Zhu B. BCG vaccines: their mechanisms of attenuation and impact on safety and protective efficacy. Hum Vaccin 2009; 5:70-8; PMID:19164935; http://dx.doi.org/10.4161/hv.5.2.7210
2. Aagaard C, Dietrich J, Doherty M, Andersen P. TB vaccines: current status and future perspectives. Immunol Cell Biol 2009; 87:279-86; PMID:19350048; http://dx.doi.org/10.1038/icb.2009.14
3. Brosch R, Gordon SV, Garnier T, Eiglmeier K, Frigui W, Valenti P, et al. Genome plasticity of BCG and impact on vaccine efficacy. Proc Natl Acad Sci U S A 2007; 104:5596-601; PMID:17372194; http://dx.doi.org/10.1073/pnas.0700869104
4. Simeone R, Bottai D, Brosch R. ESX/type VII secretion systems and their role in host-pathogen interaction. Curr Opin Microbiol 2009; 12:4-10; PMID:19155186; http://dx.doi.org/10.1016/j.mib.2008.11.003
5. Kumar D, Rao KV. Regulation between survival, persistence, and elimination of intracellular mycobacteria: a nested equilibrium of delicate balances. Microbes Infect 2011; 13:121-33; PMID:20971210; http://dx.doi.org/10.1016/j.micinf.2010.10.009
6. Deretic V, Delgado M, Vergne I, Master S, De Haro S, Ponpuak M, et al. Autophagy in immunity against mycobacterium tuberculosis: a model system to dissect immunological roles of autophagy. Curr Top Microbiol Immunol 2009; 335:169-88; PMID:19802565; http://dx.doi.org/10.1007/978-3-642-00302-8_8
7. Vergne I, Chua J, Deretic V. Mycobacterium tuberculosis phagosome maturation arrest: selective targeting of PI3P-dependent membrane trafficking. Traffic 2003; 4:600-6; PMID:12911814; http://dx.doi.org/10.1034/j.1600-0854.2003.00120.x
8. Rohde K, Yates RM, Purdy GE, Russell DG. Mycobacterium tuberculosis and the environment within the phagosome. Immunol Rev 2007; 219:37-54; PMID:17850480; http://dx.doi.org/10.1111/j.1600-065X.2007.00547.x
9. Alonso S, Pethe K, Russell DG, Purdy GE. Lysosomal killing of Mycobacterium mediated by ubiquitin-derived peptides is enhanced by autophagy. Proc Natl Acad Sci U S A 2007; 104:6031-6; PMID:17389386; http://dx.doi.org/10.1073/pnas.0700036104
10. Biswas D, Qureshi OS, Lee WY, Croudace JE, Mura M, Lammas DA. ATP-induced autophagy is associated with rapid killing of intracellular mycobacteria within human monocytes/macrophages. BMC Immunol 2008; 9:35; PMID:18627610; http://dx.doi.org/10.1186/1471-2172-9-35
11. Singh SB, Davis AS, Taylor GA, Deretic V. Human IRGM induces autophagy to eliminate intracellular mycobacteria. Science 2006; 313:1438-41; PMID:16888103; http://dx.doi.org/10.1126/science.1129577
12. Gutierrez MG, Master SS, Singh SB, Taylor GA, Colombo MI, Deretic V. Autophagy is a defense mechanism inhibiting BCG and Mycobacterium tuberculosis survival in infected macrophages. Cell 2004; 119:753-66; PMID:15607973; http://dx.doi.org/10.1016/j.cell.2004.11.038
13. Jagannath C, Lindsey DR, Dhandayuthapani S, Xu Y, Hunter RL Jr., Eissa NT. Autophagy enhances the efficacy of BCG vaccine by increasing peptide presentation in mouse dendritic cells. Nat Med 2009; 15:267-76; PMID:19252503; http://dx.doi.org/10.1038/nm.1928
14. Kumar D, Nath L, Kamal MA, Varshney A, Jain A, Singh S, et al. Genome-wide analysis of the host intracellular network that regulates survival of Mycobacterium tuberculosis. Cell 2010; 140:731-43; PMID:20211141; http://dx.doi.org/10.1016/j.cell.2010.02.012
15. Schmid D, Münz C. Innate and adaptive immunity through autophagy. Immunity 2007; 27:11-21; PMID:17663981; http://dx.doi.org/10.1016/j.immuni.2007.07.004
16. Deretic V, Levine B. Autophagy, immunity, and microbial adaptations. Cell Host Microbe 2009; 5:527-49; PMID:19527881; http://dx.doi.org/10.1016/j.chom.2009.05.016
17. Virgin HW, Levine B. Autophagy genes in immunity. Nat Immunol 2009; 10:461-70; PMID:19381141; http://dx.doi.org/10.1038/ni.1726
18. Levine B, Deretic V. Unveiling the roles of autophagy in innate and adaptive immunity. Nat Rev Immunol 2007; 7:767-77; PMID:17767194; http://dx.doi.org/10.1038/nri2161
19. Van Limbergen J, Stevens C, Nimmo ER, Wilson DC, Satsangi J. Autophagy: from basic science to clinical application. Mucosal Immunol 2009; 2:315-30; PMID:19421182; http://dx.doi.org/10.1038/mi.2009.20
20. Münz C. Enhancing immunity through autophagy. Annu Rev Immunol 2009; 27:423-49; PMID:19105657; http://dx.doi.org/10.1146/annurev.immunol.021908.132537
21. Schmid D, Pypaert M, Münz C. Antigen-loading compartments for major histocompatibility complex class II molecules continuously receive input from autophagosomes. Immunity 2007; 26:79-92; PMID:17182262; http://dx.doi.org/10.1016/j.immuni.2006.10.018
22. Giacomini E, Iona E, Ferroni L, Miettinen M, Fattorini L, Orefici G, et al. Infection of human macrophages and dendritic cells with Mycobacterium tuberculosis induces a differential cytokine gene expression that modulates T cell response. J Immunol 2001; 166:7033-41; PMID:11390447
23. Lande R, Giacomini E, Grassi T, Remoli ME, Iona E, Miettinen M, et al. IFN-alpha beta released by Mycobacterium tuberculosis-infected human dendritic cells induces the expression of CXCL10: selective recruitment of NK and activated T cells. J Immunol 2003; 170:1174-82; PMID:12538673
24. Remoli ME, Giacomini E, Lutfalla G, Dondi E, Orefici G, Battistini A, et al. Selective expression of type I IFN genes in human dendritic cells infected with Mycobacterium tuberculosis. J Immunol 2002; 169:366-74; PMID:12077266
25. Harris J, De Haro SA, Master SS, Keane J, Roberts EA, Delgado M, et al. T helper 2 cytokines inhibit autophagic control of intracellular Mycobacterium tuberculosis. Immunity 2007; 27:505-17; PMID:17892853; http://dx.doi.org/10.1016/j.immuni.2007.07.022
26. Haidinger M, Poglitsch M, Geyeregger R, Kasturi S, Zeyda M, Zlabinger GJ, et al. A versatile role of mammalian target of rapamycin in human dendritic cell function and differentiation. J Immunol 2010; 185:3919-31; PMID:20805416; http://dx.doi.org/10.4049/jimmunol.1000296
27. Hsu T, Hingley-Wilson SM, Chen B, Chen M, Dai AZ, Morin PM, et al. The primary mechanism of attenuation of bacillus Calmette-Guerin is a loss of secreted lytic function required for invasion of lung interstitial tissue. Proc Natl Acad Sci U S A 2003; 100:12420-5; PMID:14557547; http://dx.doi.org/10.1073/pnas.1635213100
28. Brodin P, de Jonge MI, Majlessi L, Leclerc C, Nilges M, Cole ST, et al. Functional analysis of early secreted antigenic target-6, the dominant T-cell antigen of Mycobacterium tuberculosis, reveals key residues involved in secretion, complex formation, virulence, and immunogenicity. J Biol Chem 2005; 280:33953-9; PMID:16048998; http://dx.doi.org/10.1074/jbc.M503515200
29. Brodin P, Majlessi L, Marsollier L, de Jonge MI, Bottai D, Demangel C, et al. Dissection of ESAT-6 system 1 of Mycobacterium tuberculosis and impact on immunogenicity and virulence. Infect Immun 2006; 74:88-98; PMID:16368961; http://dx.doi.org/10.1128/IAI.74.1.88-98.2006
30. Pym AS, Brodin P, Majlessi L, Brosch R, Demangel C, Williams A, et al. Recombinant BCG exporting ESAT-6 confers enhanced protection against tuberculosis. Nat Med 2003; 9:533-9; PMID:12692540; http://dx.doi.org/10.1038/nm859
31. Frigui W, Bottai D, Majlessi L, Monot M, Josselin E, Brodin P, et al. Control of M. tuberculosis ESAT-6 secretion and specific T cell recognition by PhoP. PLoS Pathog 2008; 4:e33; PMID:18282096; http://dx.doi.org/10.1371/journal.ppat.0040033
32. Levine B, Mizushima N, Virgin HW. Autophagy in immunity and inflammation. Nature 2011; 469:323-35; PMID:21248839; http://dx.doi.org/10.1038/nature09782
33. Remoli ME, Gafa V, Giacomini E, Severa M, Lande R, Coccia EM. IFN-beta modulates the response to TLR stimulation in human DC: involvement of IFN regulatory factor-1 (IRF-1) in IL-27 gene expression. Eur J Immunol 2007; 37:3499-508; PMID:17985330; http://dx.doi.org/10.1002/eji.200737566
34. Ní Cheallaigh C, Keane J, Lavelle EC, Hope JC, Harris J. Autophagy in the immune response to tuberculosis: clinical perspectives. Clin Exp Immunol 2011; 164:291-300; PMID:21438870; http://dx.doi.org/10.1111/j.1365-2249.2011.04381.x
35. Renshaw PS, Veverka V, Kelly G, Frenkiel TA, Williamson RA, Gordon SV, et al. Sequence-specific assignment and secondary structure determination of the 195-residue complex formed by the Mycobacterium tuberculosis proteins CFP-10 and ESAT-6. J Biomol NMR 2004; 30:225-6; PMID:15557808; http://dx.doi.org/10.1023/B:JNMR.0000048852.40853.5c
36. de Jonge MI, Pehau-Arnaudet G, Fretz MM, Romain F, Bottai D, Brodin P, et al. ESAT-6 from Mycobacterium tuberculosis dissociates from its putative chaperone CFP-10 under acidic conditions and exhibits membrane-lysing activity. J Bacteriol 2007; 189:6028-34; PMID:17557817; http://dx.doi.org/10.1128/JB.00469-07
37. Vergne I, Chua J, Lee HH, Lucas M, Belisle J, Deretic V. Mechanism of phagolysosome biogenesis block by viable Mycobacterium tuberculosis. Proc Natl Acad Sci U S A 2005; 102:4033-8; PMID:15753315; http://dx.doi.org/10.1073/pnas.0409716102
38. Shin DM, Jeon BY, Lee HM, Jin HS, Yuk JM, Song CH, et al. Mycobacterium tuberculosis eis regulates autophagy, inflammation, and cell death through redox-dependent signaling. PLoS Pathog 2010; 6:e1001230; PMID:21187903; http://dx.doi.org/10.1371/journal.ppat.1001230
39. Samuel LP, Song CH, Wei J, Roberts EA, Dahl JL, Barry CE 3rd, et al. Expression, production and release of the Eis protein by Mycobacterium tuberculosis during infection of macrophages and its effect on cytokine secretion. Microbiology 2007; 153:529-40; PMID:17259625; http://dx.doi.org/10.1099/mic.0.2006/002642-0
40. Lerena MC, Colombo MI. Mycobacterium marinum induces a marked LC3 recruitment to its containing phagosome that depends on a functional ESX-1 secretion system. Cell Microbiol 2011; 13:814-35; PMID:21447143; http://dx.doi.org/10.1111/j.1462-5822.2011.01581.x
41. Gao LY, Guo S, McLaughlin B, Morisaki H, Engel JN, Brown EJ. A mycobacterial virulence gene cluster extending RD1 is required for cytolysis, bacterial spreading and ESAT-6 secretion. Mol Microbiol 2004; 53:1677-93; PMID:15341647; http://dx.doi.org/10.1111/j.1365-2958.2004.04261.x
42. Collins CA, De Mazière A, van Dijk S, Carlsson F, Klumperman J, Brown EJ. Atg5-independent sequestration of ubiquitinated mycobacteria. PLoS Pathog 2009; 5:e1000430; PMID:19436699; http://dx.doi.org/10.1371/journal.ppat.1000430

43. Smith J, Manoranjan J, Pan M, Bohsali A, Xu J, Liu J, et al. Evidence for pore formation in host cell membranes by ESX-1-secreted ESAT-6 and its role in Mycobacterium marinum escape from the vacuole. Infect Immun 2008; 76:5478-87; PMID:18852239; http://dx.doi.org/10.1128/IAI.00614-08
44. van der Wel N, Hava D, Houben D, Fluitsma D, van Zon M, Pierson J, et al. M. tuberculosis and M. leprae translocate from the phagolysosome to the cytosol in myeloid cells. Cell 2007; 129:1287-98; PMID:17604718; http://dx.doi.org/10.1016/j.cell.2007.05.059
45. Petruccioli E, Romagnoli A, Corazzari M, Coccia EM, Butera O, Delogu G, et al. Specific T cells restore the autophagic flux inhibited by Mycobacterium tuberculosis in human primary macrophages. J Infect Dis 2012; 205:1425-35; PMID:22457295; http://dx.doi.org/10.1093/infdis/jis226
46. Saitoh T, Akira S. Regulation of innate immune responses by autophagy-related proteins. J Cell Biol 2010; 189:925-35; PMID:20548099; http://dx.doi.org/10.1083/jcb.201002021
47. Harris J, Hartman M, Roche C, Zeng SG, O'Shea A, Sharp FA, et al. Autophagy controls IL-1beta secretion by targeting pro-IL-1beta for degradation. J Biol Chem 2011; 286:9587-97; PMID:21228274; http://dx.doi.org/10.1074/jbc.M110.202911
48. Lee HK, Lund JM, Ramanathan B, Mizushima N, Iwasaki A. Autophagy-dependent viral recognition by plasmacytoid dendritic cells. Science 2007; 315:1398-401; PMID:17272685; http://dx.doi.org/10.1126/science.1136880
49. Giacomini E, Remoli ME, Gafa V, Pardini M, Fattorini L, Coccia EM. IFN-beta improves BCG immunogenicity by acting on DC maturation. J Leukoc Biol 2009; 85:462-8; PMID:19056860; http://dx.doi.org/10.1189/jlb.0908583
50. Bardarov S, Kriakov J, Carriere C, Yu S, Vaamonde C, McAdam RA, et al. Conditionally replicating mycobacteriophages: a system for transposon delivery to Mycobacterium tuberculosis. Proc Natl Acad Sci U S A 1997; 94:10961-6; PMID:9380742; http://dx.doi.org/10.1073/pnas.94.20.10961
51. Delogu G, Pusceddu C, Bua A, Fadda G, Brennan MJ, Zanetti S. Rv1818c-encoded PE_PGRS protein of Mycobacterium tuberculosis is surface exposed and influences bacterial cell structure. Mol Microbiol 2004; 52:725-33; PMID:15101979; http://dx.doi.org/10.1111/j.1365-2958.2004.04007.x
52. Rubinsztein DC, Cuervo AM, Ravikumar B, Sarkar S, Korolchuk V, Kaushik S, et al. In search of an "autophagomometer". Autophagy 2009; 5:585-9; PMID:19411822; http://dx.doi.org/10.4161/auto.5.5.8823